

Supporting information

CO₂ Electrochemical Reduction

with Zn-Al Layered Double Hydroxide-Loaded Gas-Diffusion Electrode

Ryosuke NAKAZATO^{1*§}, Keeko MATSUMOTO¹, Noboru YAMAGUCHI¹,
Margherita CAVALLO², Valentina CROCELLÀ², Francesca BONINO², Matthias
QUINTELIER³, Joke HADERMANN³, Nataly Carolina ROSERO-NAVARRO^{1,4},
Akira MIURA^{1§}, Kiyoharu TADANAGA^{1§§}

¹ *Faculty, Graduate School and School of Engineering, Hokkaido University, Kita 13,
Nishi 8, Kita-ku, Sapporo, Hokkaido 060-8628, Japan*

² *Department of Chemistry, NIS and INSTM Reference Centers, University of Turin, Via
G. Quarello 15, I-10135 and Via P. Giuria 7, I-10125 Turin, Italy*

³ *EMAT, Department of Physics, University of Antwerp, Groenenborgerlaan 171, 2020
Antwerp, Belgium*

⁴ *Instituto de Cerámica y Vidrio, CSIC, C/Kelsen 5. Campus de Cantoblanco. 28049
Madrid, Spain*

* *Corresponding author: nakazato-ryosuke@eng.hokudai.ac.jp (R. N.),
tadanaga@eng.hokudai.ac.jp (K. T.)*

§ ECSJ Active Member

§§ ECSJ Fellow

Experimental

Materials

Zinc nitrate hexahydrate ($\text{Zn}(\text{NO}_3)_2 \cdot 6\text{H}_2\text{O}$, 99.0 %), aluminium nitrate nonahydrate ($\text{Al}(\text{NO}_3)_3 \cdot 9\text{H}_2\text{O}$, 98.0 %), nickel nitrate hexahydrate ($\text{Ni}(\text{NO}_3)_2 \cdot 6\text{H}_2\text{O}$, 99.9 %), iron nitrate nonahydrate ($\text{Fe}(\text{NO}_3)_3 \cdot 9\text{H}_2\text{O}$, 99.9 %), sodium carbonate (Na_2CO_3 , 99.8 %), potassium bicarbonate (KHCO_3 , > 99.5 %), sodium hydroxide (NaOH , 97.0 %), potassium hydroxide (KOH , > 85.0 %) and potassium chloride (KCl , > 99.5 %) were purchased from FUJIFILM WAKO PURE CHEMICAL Co. Ethanol (EtOH , > 99.5 %) was purchased from Kanto Chemical Co., Inc. Water was purified by a distilled water production system (SHIMIZU SCIENTIFIC INSTRUMENTS MFG Co., Ltd.). An anion exchange membrane (AHA) was purchased from ASTOM Corp. CO_2 gas (> 99.5 %) was purchased from TAIYO NIPPON SAN SO HOKKAIDO Corp. All other solvent and chemicals in reagent grade were purchased and were used without further purification.

Preparation of M^{2+} - M^{3+} LDH ($\text{M}^{2+} = \text{Zn}$ or Ni , $\text{M}^{3+} = \text{Al}$ or Fe)

M^{2+} - M^{3+} LDHs with CO_3^{2-} anions were prepared using a facile and traditional coprecipitation process as shown in Fig. S1.¹ For the synthesis of Zn-Al LDH with CO_3^{2-} anions, an aqueous solution containing $\text{Zn}(\text{NO}_3)_2 \cdot 6\text{H}_2\text{O}$ (62 mM) and $\text{Al}(\text{NO}_3)_3 \cdot 9\text{H}_2\text{O}$ (31 mM) with $\text{Zn}^{2+}/\text{Al}^{3+} = 2.0$ was added dropwise into a 0.30 M aqueous Na_2CO_3 solution with stirring at 80 °C. The drop rate was adjusted to 2 mL min⁻¹ by using a syringe pump (SPE-1, AS ONE Corp.). The pH of the reaction mixture was adjusted to 10 by adding 2.0 M aqueous NaOH solution with a pH meter (pH700, EUTECH INSTRUMENTS Pte. Ltd.). The obtained solution was aged at room temperature for 24 h. The resulting white precipitates were filtrated, washed with distilled water, and dried at 80 °C for 24 h.

Similarly, Ni-Al LDH and Ni-Fe LDH were also prepared by replacing the $\text{Zn}(\text{NO}_3)_2 \cdot 6\text{H}_2\text{O}$ and $\text{Al}(\text{NO}_3)_3 \cdot 9\text{H}_2\text{O}$ with the corresponding $\text{Ni}(\text{NO}_3)_2 \cdot 6\text{H}_2\text{O}$ and $\text{Fe}(\text{NO}_3)_3 \cdot 9\text{H}_2\text{O}$, respectively.

The product was characterized by X-ray diffraction (XRD), scanning transmission electron microscopy coupled with energy-dispersive X-ray spectrometry (STEM-EDX), bright field transmission electron microscopy (BF-TEM) and attenuated total reflectance infrared spectroscopy (ATR-IR, Bruker Invenio Fourier transform spectrometer). XRD patterns ($\text{CuK}\alpha$) were obtained using an XRD diffractometer (Mini Flex 600, Rigaku Corp.) to identify the crystalline phase. The sample morphology and chemical composition were determined by a field emission SEM (FE-SEM: JSM-7001FA, JEOL Ltd.), BF-TEM (Thermo Fisher Titan microscope, operated at 300 kV, image corrected and equipped with a Gatan K2 DED) and STEM-EDX (Thermo Fisher Tecnai Osiris microscope, operated at 200 kV and equipped with a Super X detector). CO_2 adsorption was investigated by in-situ ATR-IR measurement performed with a Bruker Invenio Fourier transform spectrometer, equipped with a mercury cadmium telluride detector operated at liquid nitrogen temperature using a commercial horizontal ATR mirror unit and cell (PIKE TECHNOLOGIES). Each spectrum consisted of the average of 32 scans (64 for the background spectrum). Each LDH sample, firstly suspended in water (~ 15 mg per 0.5 mL of Deionized H_2O), was deposited on an AMTIR single crystal internal reflection element ($80 \times 10 \times 4$ mm, 45° , SPECAC Ltd.) and dried overnight. H_2O in liquid phase saturated with N_2 was circulated inside the cell, over the deposited sample, at room temperature for 30 minutes to verify the stability of the deposition. The inlet gas was consequently switched to CO_2 and a CO_2 -saturated liquid H_2O flow was circulated over the sample for other 30 minutes. Prior to each experiment a fresh LDH sample was deposited on the crystal.

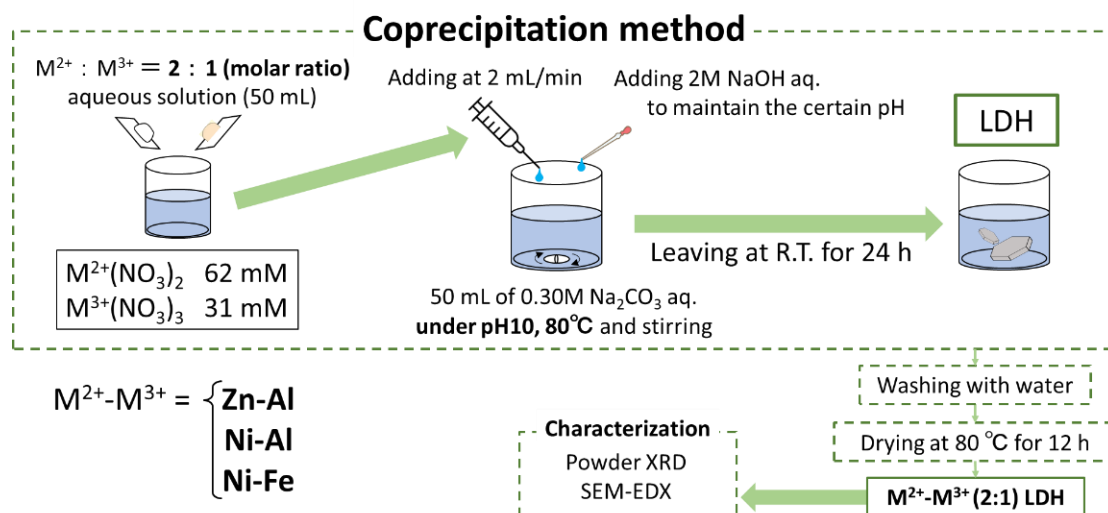


Figure S1. Synthesis scheme of $M^{2+}-M^{3+}$ LDH by coprecipitation method in this study.

Preparation of the LDH-loaded GDE as a working electrode

The LDH-loaded GDE was prepared by simple drop-casting of the catalyst ink on a gas-diffusion layer (GDL: Sigracet 36BB, SGL CARBON JAPAN Ltd.). The catalyst inks were prepared by mixing 4 mg of LDH ground for 30 min with 1 mg of the conductive aid (carbon black: Vulcan XC72, CABOT Corp.) and 30 μL of the binder (Nafion solution, SIGMA-ALDRICH Co. LLC) in 570 μL of ethanol and sonicating for 10 min. The catalyst ink was drop-casted to the GDL on a hot plate pre-heated at 80 °C. The ink coating area was 1.89 cm^2 , whose shape was a 1.55 cm diameter circle and the loading level of the LDH was 2.1 mg cm^{-2} . The LDH-loaded GDE was further dried at 80 °C for at least 30 min to remove the solvents. For the Zn-Al LDH-loaded LDH, the macro-scale morphology was observed by scanning electron microscopy coupled with energy-dispersive X-ray spectrometry (SEM-EDX, TM3030, Hitachi Ltd.; SwiftED3000, Oxford Instruments). As a control sample, the GDE without LDHs was prepared by using the ink mixed with 1 mg of the conductive aid and 30 μL of the binder in 570 μL of ethanol.

Gas-phase CO₂ER experiment

Gas-phase CO₂ER with the LDH-loaded GDE was carried out by using a custom-made three-electrode setup composed of a three-compartment cell as shown in Fig. S2. The cathodic and anodic compartments were separated by a piece of the anion exchange membrane to avoid the unexpected influence of the oxidation reaction taking place on the counter electrode. The LDH-loaded GDE and a platinum mesh electrode (35 × 25 mm, LAKE SHORE CRVOTRONICS Inc.) were used as working and counter electrodes, respectively. Ag/AgCl (3.0 M KCl, BAS Inc.) or Hg/HgO (1.0 M NaOH, BAS Inc.) electrodes were used as reference under near-neutral pH condition (pH: 6.5 or 8.2) or a strong alkaline one (pH: 14), respectively. Aqueous solutions (1.0 M) of KHCO₃, KCl, or KOH were used as catholytes for pH 6.5, 8.2, or 14 conditions, respectively. A 1.0 M aqueous KOH solution was used as an anolyte for all pH conditions. The pH of each electrolyte was measured with a pH meter (pH700, EUTECH INSTRUMENTS Pte. Ltd.). The CO₂ gas flowed with a 50 mL min⁻¹ flow rate and 0.10 MPa inlet pressure to the cathodic compartment, while the solution in the reference electrode compartment was stirred at 600 rpm with a PTFE stirring bar. Under the above conditions, CO₂ electrolysis for 10 min was performed by applying a voltage with an electrochemical analyzer (SL1287, SOLARTRON). Gas-phase products were detected by gas chromatography techniques (GC-2014, SHIMADZU Corp.; carrier gas: nitrogen, flow rate: 10 mL min⁻¹, pressure: 53.2 kPa, vaporization chamber temperature: 120 °C). For the detection of hydrogen (H₂), Molecular Sieve 5A (GL SCIENCES Inc.; column temperature: 50 °C, injected sample volume: 1 mL) and a thermal conductivity detector (TCD, SHIMADZU Corp.; detector temperature: 120 °C) were used. For the detection of CO and gaseous hydrocarbons, PoraPak N (GL SCIENCES Inc.; column temperature: 50 °C, injected sample volume: 1 mL) for a flame ionization detector (FID, SHIMADZU Corp.; detector temperature: 120 °C) were used. liquid phase products were analyzed using ¹H nuclear magnetic resonance (¹H-NMR) spectroscopy (400 MHz, ECZ400S, JEOL Ltd.).

Electrode potentials in the study were converted to the reversible hydrogen electrode (RHE) or the standard hydrogen electrode (SHE) according to the following equations: $E_{\text{RHE}} = E_{\text{SHE}} + 0.059 \times \text{pH}$, $E_{\text{SHE}} = E_{\text{Ag/AgCl}} + 0.222 \text{ V} = E_{\text{Hg/HgO}} + 1.760 \text{ V}$. All potentials and voltages in this work were evaluated without iR calibration. The Faradaic efficiency (FE) for CO and H₂ was calculated based on the equation²:

$$FE = \frac{2VprF}{IRT}$$

Where V was the volume concentration of CO or H₂ in the produced gas from the reaction cell. I (mA) was the average current during the reaction, and r was the CO₂ flow rate (m³ s⁻¹) at ambient temperature and pressure. For the other constants in the formula, p was $1.013 \times 10^5 \text{ Pa}$, F was 96485 C mol^{-1} , R was $8.3145 \text{ J mol}^{-1} \text{ K}^{-1}$, and T was 298 K .

Assuming that a zinc atom was the active center, turnover frequency (TOF) and turnover number (TON) for CO was calculated based on the equation²:

$$TOF (\text{s}^{-1}) = \frac{j_{\text{CO}} / F}{n (M_{\text{LDH}} / W_{\text{LDH}})} , \quad TON = TOF \times t$$

Where j_{CO} was the partial current density (mA cm⁻²) for CO, F was 96485 C mol^{-1} , and n was the number of electrons transferred for product formation, which was 2 for CO formation. M_{LDH} was the loading level of the LDH (2.1 mg cm⁻²), and W_{LDH} was the formula weight (145 g/mol) of LDH for $[\text{Zn}^{2+}_1\text{Al}^{3+}_{0.5}(\text{OH})_3]^{0.5+} [(\text{CO}_3^{2-})_{0.25}]^{0.5-}$. t was the reaction duration, which was 600 s for this study.

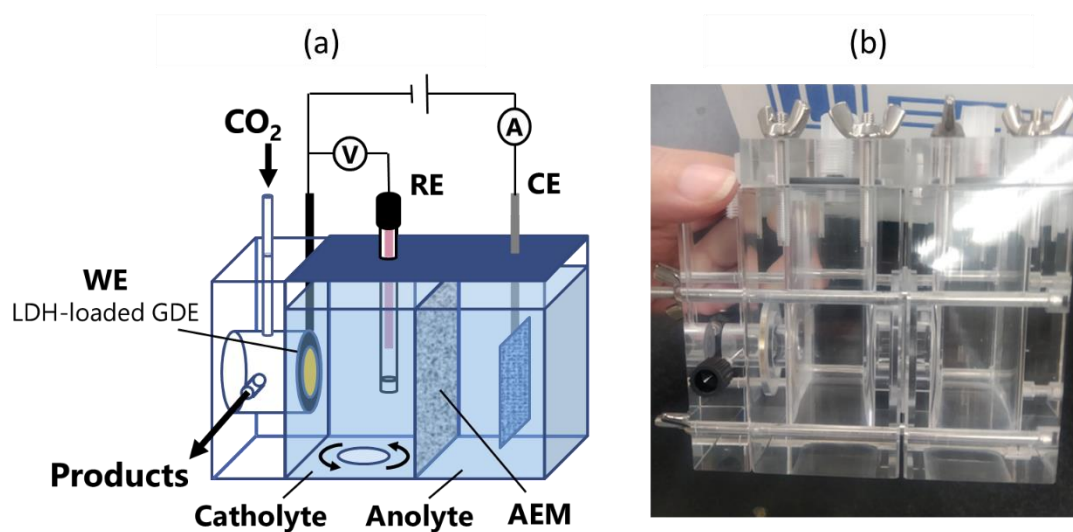


Figure S2. Custom-made three-electrode setup composed of a three-compartment cell for electrocatalytic CO₂ER with the LDH-loaded GDE (WE: working electrode, CE: counter electrode, RE: reference electrode, AEM: anion exchange membrane).

Supplementary results

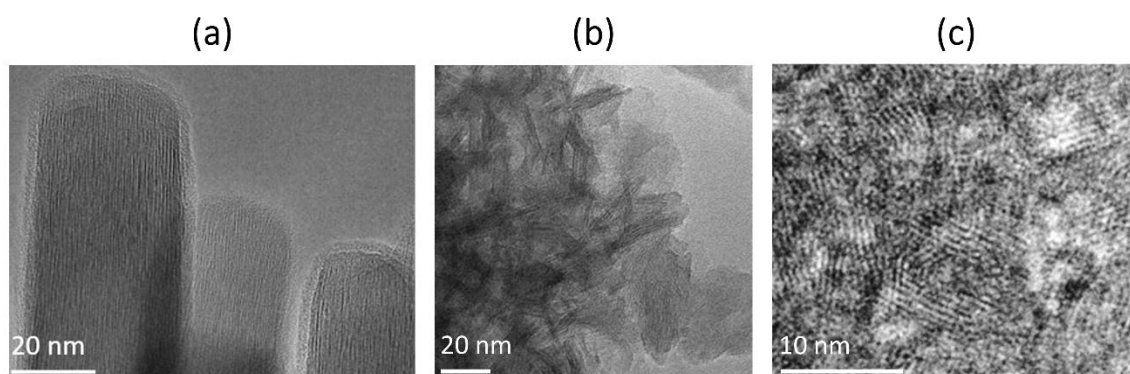


Figure S3. BF-TEM image of (a) Zn-Al LDH, (b) Ni-Al LDH and (c) Ni-Fe LDH.

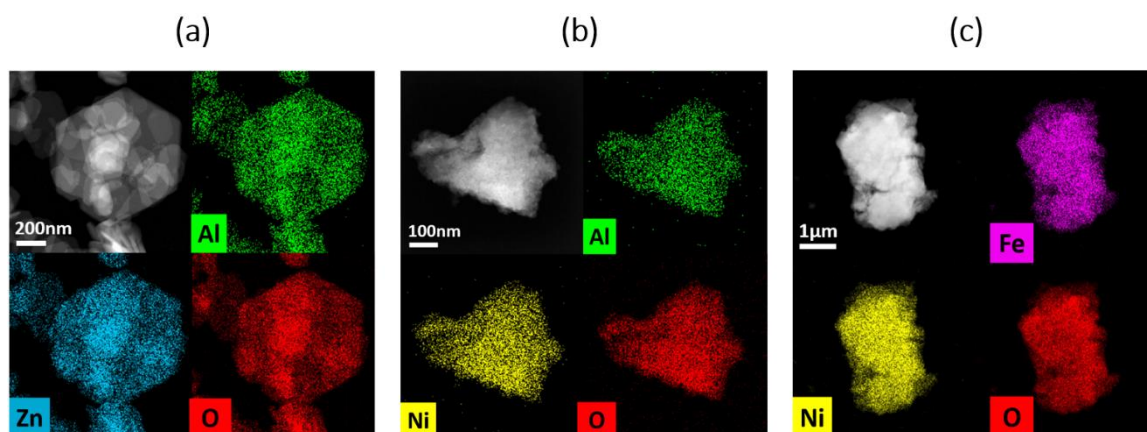


Figure S4. High-angle annular dark field (HAADF)-STEM images and EDX mapping (a) Zn-Al LDH, (b) Ni-Al LDH and (c) Ni-Fe LDH.

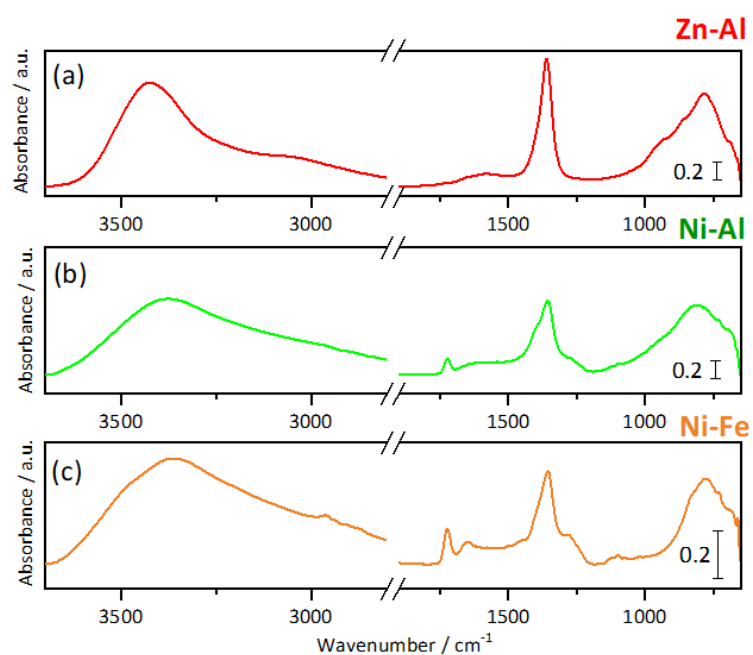


Figure S5. ATR-IR spectra in the 3700-650 cm^{-1} spectral region of dry (a) Zn-Al LDH, (b) Ni-Al LDH and (c) Ni-Fe LDH.

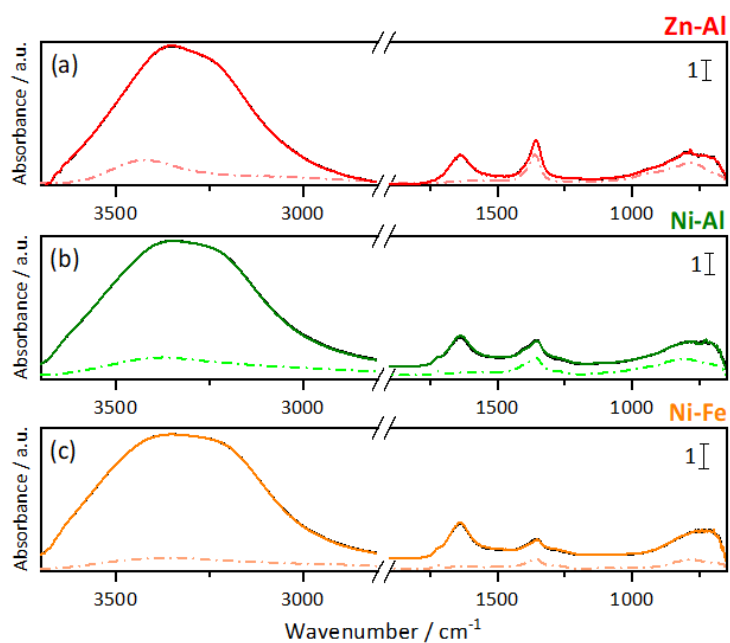


Figure S6. In-situ ATR-IR spectra in the 3600-650 cm^{-1} spectral region of: (a) Zn-Al LDH, (b) Ni-Al LDH and (c) Ni-Fe LDH. Dotted colored, black, and continuous colored curves represent the dry, wet N_2 -saturated, and wet CO_2 -saturated samples, respectively.

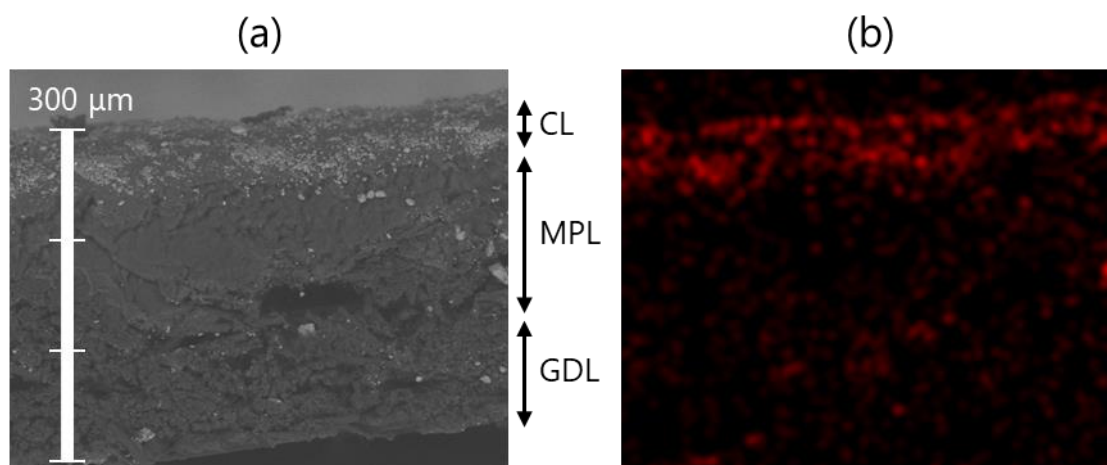


Figure S7. (a) The cross-sectional SEM image (CL: catalyst layer, MPL: micro-porous layer, GDL: gas-diffusion layer) and (b) EDX mapping of Zn for the Zn-Al LDH.

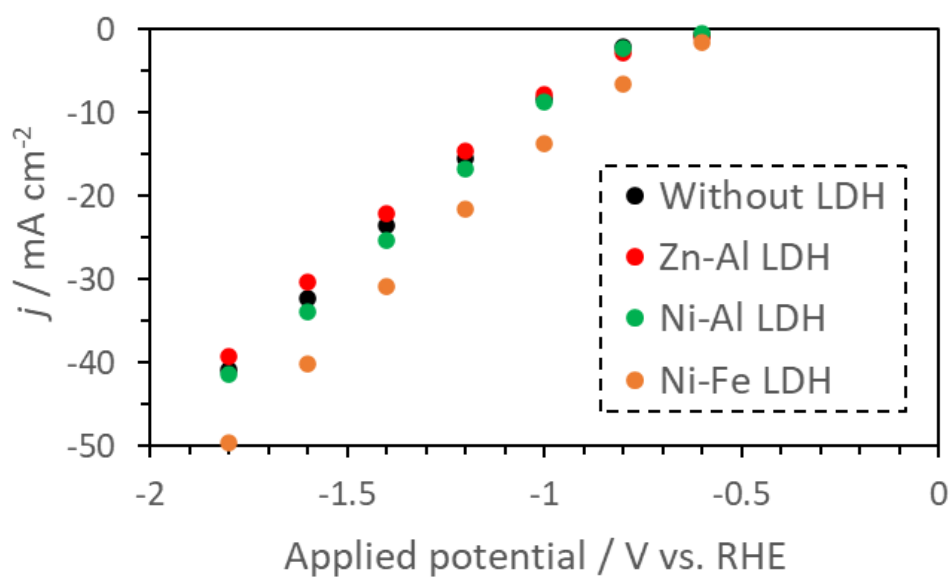


Figure S8. Applied potential dependence of current density (j) for CO₂ER in 1.0M aqueous KHCO₃ solution using each cathode with Zn-Al LDH (red), Ni-Al LDH (green) and Ni-Fe LDH (orange), and without LDH (black).

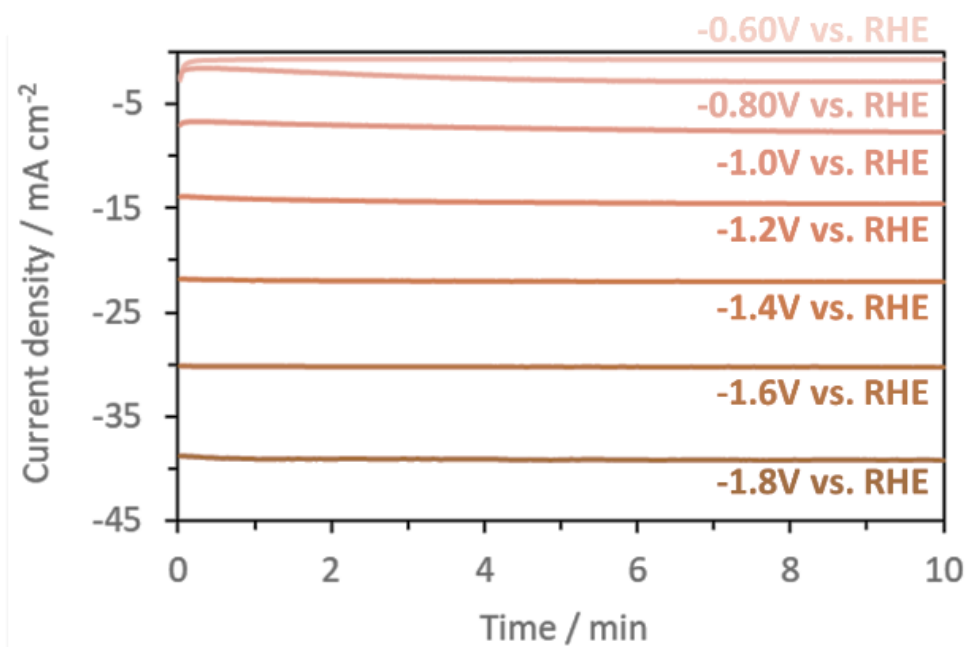


Figure S9. Applied potential dependence of chronoamperogram for CO₂ER with Zn-Al LDH in 1.0 M aqueous KHCO₃ solution.

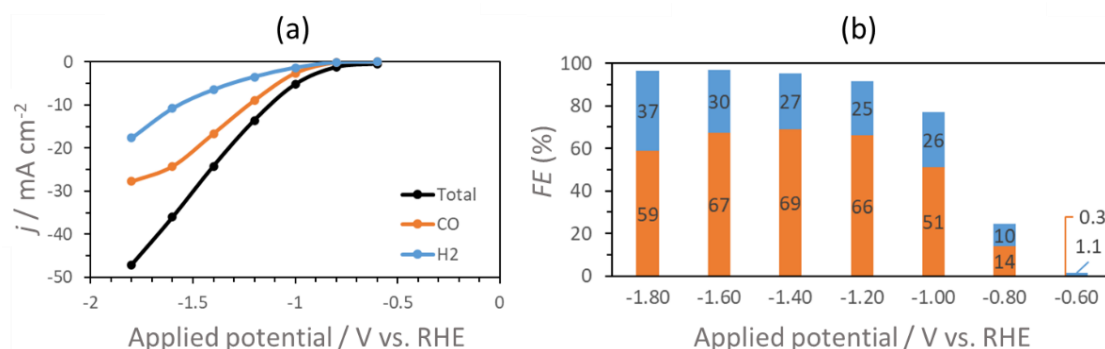


Figure S10. (a) Applied potential dependence of current density (j) and (b) Faradaic efficiency (FE; orange bar: CO, blue bar: H₂) for CO₂ER with Zn-Al LDH in 1.0 M KCl aqueous solution.

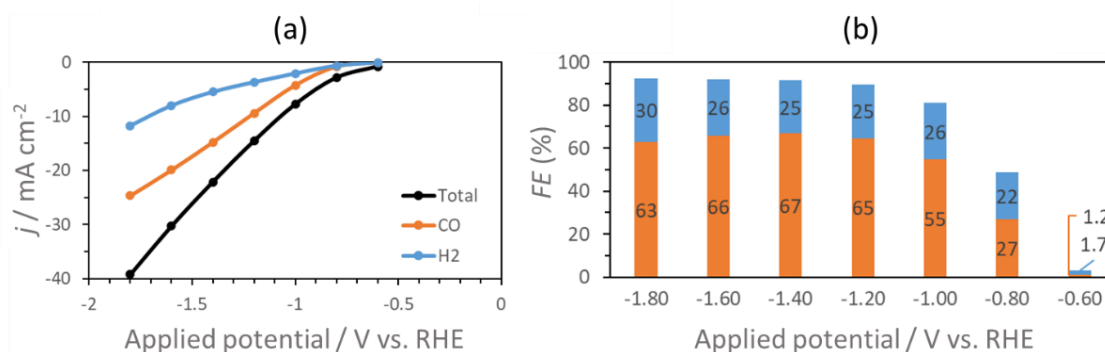


Figure S11. (a) Applied potential dependence of current density (j) and (b) Faradaic efficiency (FE; orange bar: CO, blue bar: H₂) for CO₂ER with Zn-Al LDH in 1.0 M KHCO₃ aqueous solution.

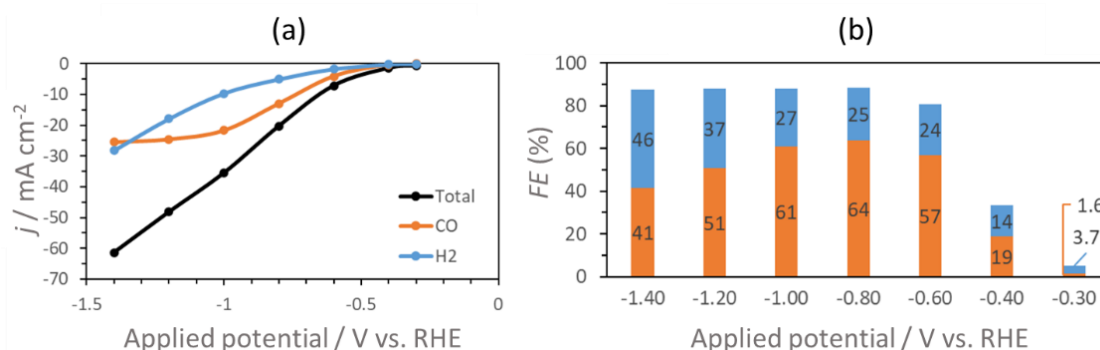


Figure S12. (a) Applied potential dependence of current density (j) and (b) Faradaic efficiency (FE; orange bar: CO, blue bar: H₂) for CO₂ER with Zn-Al LDH in 1.0 M KOH aqueous solution.

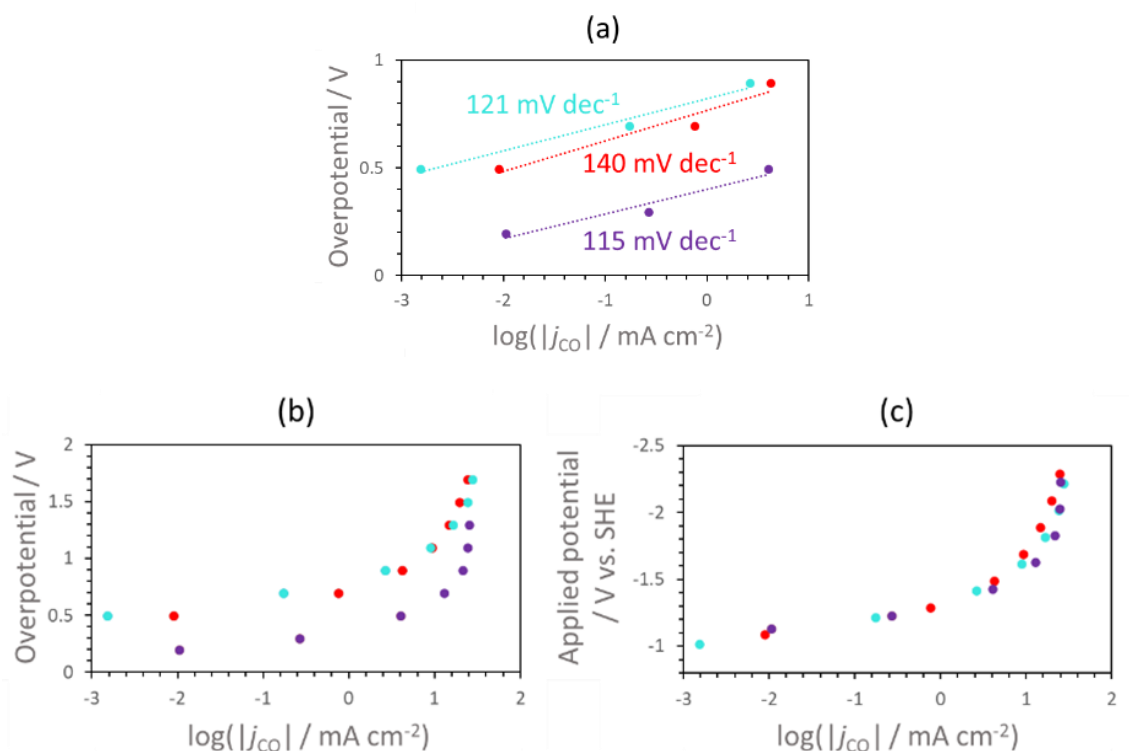


Figure S13. Tafel plot of CO formation in (a) the electron transfer rate-limiting range and (b) overall range, and (c) applied potential vs. SHE versus CO partial current density (j_{CO}) for CO_2ER with Zn-Al LDH in each 1.0 M aqueous solution of KCl (cyan plots and dotted line), KHCO_3 (red plots and dotted line) and KOH (purple plots and dotted line).

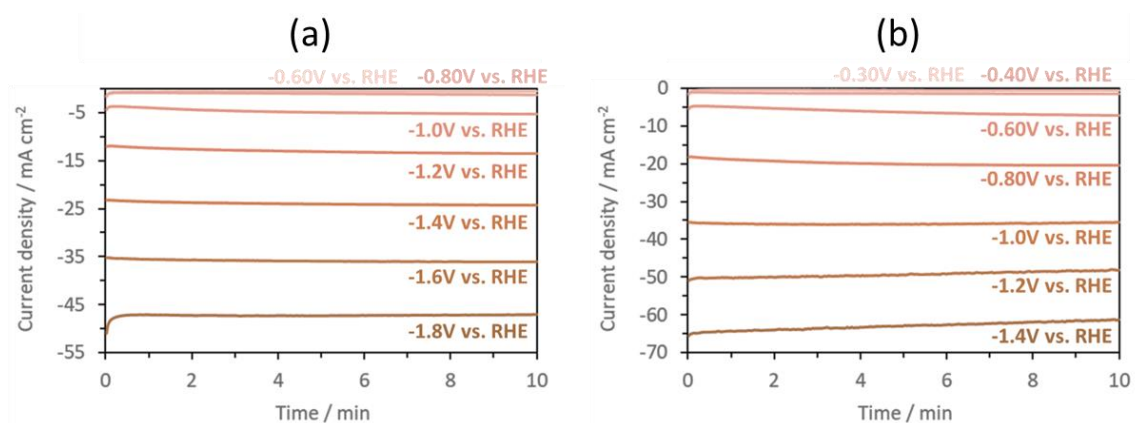


Figure S14. Applied potential dependence of chronoamperogram for CO_2ER with Zn-Al LDH in 1.0 M aqueous solution of (a) KCl and (b) KOH.

Table S1. Summary of Current Density (j) and Faradaic Efficiency (FE) for Gas-Phase and Liquid-Phase CO₂ER with Zn-Al LDH

Experimental condition	Applied potential / V vs. RHE	Partial current density for CO formation ($ j_{CO} $) / mA cm ⁻²	Faradaic efficiency for CO formation (FE_{CO}) (%)	Faradaic efficiency for CO and H ₂ formation (FE_{CO+H_2}) (%)
Gas-phase CO ₂ ER in 1.0 M KCl	-0.60	1.5×10^{-3}	0.33	1.4
	-1.0	2.7	51	77
	-1.4	17	69	96
Gas-phase CO ₂ ER in 1.0 M KHCO ₃	-0.60	9.0×10^{-3}	1.2	2.9
	-1.0	4.2	55	81
	-1.4	15	67	92
Gas-phase CO ₂ ER in 1.0 M KOH	-0.60	4.1	57	81
	-1.0	22	61	88
	-1.4	25	41	87
Liquid-phase CO ₂ ER in 0.10 M KHCO ₃	-0.60	3.4×10^{-3}	0.63	0.63
	-1.0	1.9	38	76
	-1.4	12	77	94

References

1. M. Yasaei, M. Khakbiz, A. Zamanian, and E. Ghasemi, *Mater. Sci. Eng. C*, **103**, 109816 (2019).
2. X. Wu, J. W. Sun, P. F. Liu, J. Y. Zhao, Y. Liu, L. Guo, S. Dai, H. G. Yang, and H. Zhao, *Adv. Funct. Mater.*, **32**, 2107301 (2022).
3. N. Yamaguchi, R. Nakazato, K. Matsumoto, M. Kakesu, N. C. Rosero-Navarro, A. Miura, and K. Tadanaga, *J. Asian Ceram. Soc.*, **11**, 406 (2023).